Comput. Methods Appl. Mech. Engrg. 199 (2010) 648–659

Contents lists available at ScienceDirect

Comput. Methods Appl. Mech. Engrg.

journal homepage: www.elsevier.com/locate/cma

Quadrature-rule type approximations to the quasicontinuum method for long-range interatomic interactions ☆

Yanzhi Zhang *, Max Gunzburger

Department of Scientific Computing, Florida State University, Tallahassee, FL 32306-4120, USA

ARTICLE INFO

Article history:
Received 13 May 2009
Received in revised form 18 September 2009
Accepted 23 October 2009
Available online 31 October 2009

Keywords:
Atomistic models
Quasicontinuum method
Quadrature-rule type approximation
Long-range interactions
Coulomb potential

ABSTRACT

A quadrature-rule type method is presented to approximate the quasicontinuum method for atomistic mechanics. For both the short-range and long-range interaction cases, the complexity of this method depends on the number of representative particles but not on the total number of particles. Simple analysis and numerical experiments are provided to illustrate the accuracy and performance of the method. It is shown that, for the same accuracy, the quadrature-rule type method is much less costly than the quasicontinuum method.

1. Introduction

We begin by stating the molecular statics problem we wish to solve. Consider a crystal with N particles and let[1] $\mathcal{N} = \{1, \dots, N\}$ denote the index set of all particles. Denote by $\mathbf{X}_\alpha, \mathbf{x}_\alpha \in \mathbb{R}^d$ the positions of particle $\alpha \in \mathcal{N}$ in the reference and deformed configurations, respectively, where $d = 1$, 2, or 3 denotes the spatial dimension. In practice, the position of some particles, e.g., the particles located near or on parts of the boundary, may be specified. Thus we denote by $\mathcal{N}_f \subset \mathcal{N}$ the index set of the particles whose positions are specified through

$$\mathbf{x}_\alpha = \mathbf{x}_\alpha^0 \quad \text{for } \alpha \in \mathcal{N}_f, \tag{1.1}$$

where $\mathbf{x}_\alpha^0$ is a given position vector. Let $\mathcal{N}_a = \mathcal{N} \setminus \mathcal{N}_f$ so that $\mathcal{N}_a$ is the index set of the remaining particles, i.e., the particles whose positions are not specified.

The total potential energy is defined by

$$\Phi(\{\mathbf{x}_\alpha\}_{\alpha\in\mathcal{N}}) = \Phi^a(\{\mathbf{x}_\alpha\}_{\alpha\in\mathcal{N}}) + \Phi^e(\{\mathbf{x}_\alpha\}_{\alpha\in\mathcal{N}}), \tag{1.2}$$

where Φ^a denotes the potential energy due to the interaction between particles and Φ^e is a conservative external potential. We assume that the potential energy Φ^a can be given as a sum of pairwise interaction potentials each of which depends only on the position of the corresponding pair of particles, i.e.,

$$\Phi^a(\{\mathbf{x}_\alpha\}_{\alpha\in\mathcal{N}}) = \frac{1}{2}\sum_{\alpha\in\mathcal{N}}\sum_{\beta\in\mathcal{N},\beta\neq\alpha} \Phi^a_{\alpha,\beta}(\mathbf{x}_\alpha, \mathbf{x}_\beta), \tag{1.3}$$

where $\Phi^a_{\alpha,\beta} = \Phi^a_{\beta,\alpha}$ denotes the interaction energy between the particles α and β. In addition, we assume that the external potential Φ^e can be expressed as a sum of the potential energies of the external force acting on each particle and that the latter depends only on the position of the corresponding particle, i.e.,

$$\Phi^e(\{\mathbf{x}_\alpha\}_{\alpha\in\mathcal{N}}) = \sum_{\alpha\in\mathcal{N}} \Phi^e_\alpha(\mathbf{x}_\alpha). \tag{1.4}$$

Thus the total potential energy in (1.2) can be expressed as

$$\Phi(\{\mathbf{x}_\alpha\}_{\alpha\in\mathcal{N}}) = \frac{1}{2}\sum_{\alpha\in\mathcal{N}}\sum_{\beta\in\mathcal{N},\beta\neq\alpha} \Phi^a_{\alpha,\beta}(\mathbf{x}_\alpha, \mathbf{x}_\beta) + \sum_{\alpha\in\mathcal{N}} \Phi^e_\alpha(\mathbf{x}_\alpha). \tag{1.5}$$

To determine stable equilibrium configurations, we minimize the total energy $\Phi(\{\mathbf{x}_\alpha\}_{\alpha\in\mathcal{N}})$ in (1.5) subject to (1.1), i.e., we solve the problem

$$\min_{\mathbf{x}_\alpha, \alpha\in\mathcal{N}_a} \Phi(\{\mathbf{x}_\beta\}_{\beta\in\mathcal{N}}) \quad \text{subject to} \quad (1.1) \tag{1.6}$$

☆ This work was supported by the US Department of Energy under Grant Number DE-FG02-05ER25698 as part of the office of Science's "Multiscale Mathematics" program.

* Corresponding author.
E-mail addresses: yzhang5@fsu.edu (Y. Zhang), gunzburg@fsu.edu (M. Gunzburger).

[1] We use calligraphic letters, e.g., $\mathcal{N}$, to represent index sets and the corresponding Roman letters, e.g., N for their cardinality.

0045-7825/$ - see front matter © 2009 Elsevier B.V. All rights reserved.
doi:10.1016/j.cma.2009.10.015

or, equivalently,[2]

$$\frac{\partial \Phi}{\partial \mathbf{x}_\alpha}(\{\mathbf{x}_\beta\}_{\beta\in\mathcal{N}}) = \mathbf{0} \quad \text{for } \alpha \in \mathcal{N}_a \quad \text{and} \quad \mathbf{x}_\alpha = \mathbf{x}_\alpha^0 \quad \text{for } \alpha \in \mathcal{N}_f. \tag{1.7}$$

We see that, after substituting (1.1), (1.7) becomes a system of dN_a equations in dN_a unknowns $\mathbf{x}_\alpha$, $\alpha \in \mathcal{N}_a$. Usually, the number N_a is of the order of N, which is a huge number so that solving the whole system (1.7) (the full atomistic model) is impractical.

On the other hand, many practical problems require full atomistic resolution only in small regions where defects occur. To simplify the large atomistic model, the quasicontinuum (QC) method was proposed in [1,2]. Instead of treating all particles, the QC method considers only a small set of representative particles and approximates the energy of the whole system in term of the representative particles. As a result, it involves significantly fewer degrees of freedom compared to the full atomistic system (1.7). Recently, the QC method has become a popular multiscale method for material modeling and simulation; many implementations, enhancements, extensions, and applications of the QC method are addressed in, e.g., [3–18]. Analysis of the QC method and its variants can be found in, e.g., [4,6,8,10–12,14].

Although it has fewer degrees of freedom than the full atomistic model, the original QC method, in its raw form, still involves calculations over the full atomistic lattices so that the work needed to obtain a solution is still dependent on the total number of particles N [12,1,2]. To avoid this, many methods have been proposed to approximate the QC method, e.g., node-based summation rules [12], cluster summation rules [12], and quadrature-rule type methods [19]. Provided that the interatomic interactions are short-ranged, the computational complexities of all these methods are independent of N, the total number of particles. However, many materials exhibit long-range interactions [20]. Although numerical experiments show that both the cluster summation rule and the quadrature-rule type methods are quite stable and accurate for the case of short-range interactions [12,19], they are not effective for the long-range case. This is because, in the long-range interaction case, these methods still have computational complexities that depend on the total number of particles.

Coulomb forces are the prime example of a long-range interaction; such forces are present in many materials including bio-molecules. Due to the very large set of applications in which Coulombic interactions play a central role, it is not surprising that many methods have been developed with the aim of reducing the complexity of molecular dynamic calculations for this case; see, e.g., [21–24] for methods that are not connected to the QC method. However, as is the case for cluster summation approximations to the QC method [12], none of these has complexity that is independent of the total number of particles. For example, the method of [21] has complexity of $O(N^{3/2})$, that used in [22,23] is at best of $O(N)$, and that of [24] reduces the complexity only by a factor of 3–5, i.e., the dependence on N remains unchanged. The QC–QR method developed in this paper has complexity for the Coulombic interaction case, indeed for any long-range as well as short-range interaction problem, that is independent of the total number of particles.

In [19], quadrature-rule (QC–QR) type approximations to the quasicontinuum (QC) method were presented and tested for the case of short-range interactions. The development of the method for the case of long-range interactions requires several algorithmic innovations. The aim of this paper is to present, discuss, analyze, and illustrate these innovations. However, in several places, some aspects of the method in this paper are shared with those in [19] so that we rely on that paper for some algorithmic details.[3]

The paper is organized as follows: in Section 2, we review the QC method for molecular statics and introduce the notations used in subsequent sections. In Section 3, we provide a detailed description of the QC–QR method and, in Section 4, an analysis of its accuracy and complexity is presented. Numerical examples are presented in Section 5 to illustrate the performance characteristics of the QC–QR method; in particular, we illustrate that indeed the complexity of the QC–QR method is independent of the total number of particles, even for the long-range interaction case. In Section 6, we give a brief summary and discussion of follow-up work.

2. The quasicontinuum (QC) method

Let $\widetilde{\mathcal{N}}_r \subset \mathcal{N}$ denote the index set of the *representative particles*. The selection of the representative particles is based on the local variation of the fields; see [12] for the details. Typically, since the particles having specified positions may provide important information of the system, e.g., the "boundary" condition, one should choose all of them to be among the representative particles so that $\mathcal{N}_f \subset \widetilde{\mathcal{N}}_r$. Then denote $\mathcal{N}_r = \widetilde{\mathcal{N}}_r \setminus \mathcal{N}_f$ as the index set of the remaining representative particles whose positions are not specified through (1.1).

In the reference configuration, construct a triangulation $\mathsf{T}_h = \{\Delta_t\}_{t=1}^T$ which consists of simplices having the representative particles as vertices. Let $\{\psi_j^h(\mathbf{X})\}_{j\in\widetilde{\mathcal{N}}_r}$ denote a collection of basis functions corresponding to the triangulation T_h. In particular, we choose $\psi_j^h(\cdot)$ to be a continuous, piecewise linear polynomial with support restricted to the simplices having $\mathbf{X}_j$ as a vertex [25]. Thus if $\mathcal{T}_j = \{t \in \{1,\dots,T\} | \mathbf{X}_j \in \overline{\Delta}_t\}$, i.e., $\mathcal{T}_j$ is the index set of simplices which have the particle $\mathbf{X}_j$ serving as a vertex, we have

$$\psi_j^h(\mathbf{X}) = 0 \quad \text{for } \mathbf{X} \in \overline{\Delta}_t \quad \text{but } t \notin \mathcal{T}_j.$$

Based on the Cauchy–Born hypothesis, we assume that the position of particle $\alpha \in \mathcal{N}_a$ can be approximated through interpolation of the (approximate) positions of the representative particles, i.e.,

$$\mathbf{x}_\alpha^h = \sum_{j\in\widetilde{\mathcal{N}}_r} \mathbf{x}_j^h\ \psi_j^h(\mathbf{X}_\alpha) \approx \mathbf{x}_\alpha \quad \text{for } \alpha \in \mathcal{N}_a, \tag{2.1}$$

where $\mathbf{x}_j^h$ is the (approximate) position of the representative particle $j \in \widetilde{\mathcal{N}}_r$. In fact, (2.1) holds for any particle $\alpha \in \mathcal{N}$, including the representative particles. Substituting (2.1) into the total potential energy in (1.5), we have

$$\begin{aligned}\Phi^h(\{\mathbf{x}_j^h\}_{j\in\widetilde{\mathcal{N}}_r}) &= \Phi(\{\mathbf{x}_\alpha^h\}_{\alpha\in\mathcal{N}}) \\ &= \frac{1}{2}\sum_{\alpha\in\mathcal{N}}\sum_{\beta\in\mathcal{N},\beta\neq\alpha} \Phi_{\alpha,\beta}^a(\mathbf{x}_\alpha^h, \mathbf{x}_\beta^h) \\ &\quad + \sum_{\alpha\in\mathcal{N}} \Phi_\alpha^e(\mathbf{x}_\alpha^h) \approx \Phi(\{\mathbf{x}_\alpha\}_{\alpha\in\mathcal{N}}).\end{aligned} \tag{2.2}$$

Due to (2.1), Φ^h is indeed a function of the (approximate) positions of the representative particles. Thus, the only degrees of freedom appearing in Φ^h are the positions of the representative particles whose positions are not specified through (1.1). To determine these degrees of freedom, we solve the minimization problem

$$\min_{\mathbf{x}_j^h\, j\in\mathcal{N}_r} \Phi^h(\{\mathbf{x}_k^h\}_{k\in\widetilde{\mathcal{N}}_r}) \quad \text{subject to} \quad (1.1).$$

Equivalently, we solve the system

[2] The notation $\partial\Phi/\partial\mathbf{y}$ denotes the d-vector $\nabla_{\mathbf{y}}\Phi$ having components $\partial\Phi/\partial y_k, k = 1,\dots,d$.

[3] We note that extensive comparisons of the QC–QR method and the cluster summation method [12] are given in [19] for the case of short-range interactions.

$$\begin{cases} \frac{\partial \Phi^h}{\partial \mathbf{x}_j^h}\left(\{\mathbf{x}_i^h\}_{i\in\widetilde{\mathcal{N}}_r}\right) = \sum_{\alpha\in\mathcal{N}_a} \frac{\partial \Phi}{\partial \mathbf{x}_\alpha^h}\left(\{\mathbf{x}_\beta^h\}_{\beta\in\mathcal{N}}\right)\psi_j^h(\mathbf{X}_\alpha) = \mathbf{0} \quad \text{for } j\in\mathcal{N}_r \\ \text{where } \mathbf{x}_\alpha^h = \mathbf{x}_\alpha^0 \quad \text{if } \alpha\in\mathcal{N}_f; \quad \mathbf{x}_\alpha^h = \sum_{k\in\widetilde{\mathcal{N}}_r} \mathbf{x}_k^h\psi_k^h(\mathbf{X}_\alpha) \quad \text{if } \alpha\in\mathcal{N}_a. \end{cases} \tag{2.3}$$

Denote by

$$\mathcal{N}_j = \left\{\alpha\in\mathcal{N}_a | \mathbf{X}_\alpha \in \operatorname{supp}\left(\psi_j^h(\mathbf{X})\right)\right\}$$

the index set of the particles that are located (in the reference configuration) within the support of the basis function $\psi_j^h(\cdot)$, but whose positions are not specified by (1.1). Thus for any particle $\alpha\in\mathcal{N}_a\setminus\mathcal{N}_j$, we have that $\psi_j^h(\mathbf{X}_\alpha)=0$. Then the system (2.3) reduces to [19]

$$\begin{cases} \sum_{\alpha\in\mathcal{N}_j}\psi_j^h(\mathbf{X}_\alpha)\left(\sum_{\beta\in\mathcal{N},\beta\neq\alpha}\mathbf{f}_{\alpha,\beta}^a(\mathbf{x}_\alpha^h,\mathbf{x}_\beta^h)\right) + \sum_{\alpha\in\mathcal{N}_j}\psi_j^h(\mathbf{X}_\alpha)\mathbf{f}_\alpha^e(\mathbf{x}_\alpha^h) = \mathbf{0} \quad j\in\mathcal{N}_r \\ \text{where } \mathbf{x}_\alpha^h = \mathbf{x}_\alpha^0 \quad \text{if } \alpha\in\mathcal{N}_f; \quad \mathbf{x}_\alpha^h = \sum_{k\in\widetilde{\mathcal{N}}_r}\mathbf{x}_k^h\psi_k^h(\mathbf{X}_\alpha) \quad \text{if } \alpha\in\mathcal{N}_a, \end{cases} \tag{2.4}$$

where the function

$$\mathbf{f}_{\alpha,\beta}^a(\mathbf{x}_\alpha,\mathbf{x}_\beta) = -\frac{\partial \Phi_{\alpha,\beta}^a(\mathbf{x}_\alpha,\mathbf{x}_\beta)}{\partial \mathbf{x}_\alpha} \quad \text{for } \alpha,\beta\in\mathcal{N} \tag{2.5}$$

defines the force acting on particle α due to its interaction with particle β and the external force on particle α is defined by

$$\mathbf{f}_\alpha^e(\mathbf{x}_\alpha) = -\frac{\partial \Phi_\alpha^e(\mathbf{x}_\alpha)}{\partial \mathbf{x}_\alpha} \quad \text{for } \alpha\in\mathcal{N}. \tag{2.6}$$

In the system (2.4), there are dN_r equations in the same number of unknowns $\mathbf{x}_j^h, j\in\mathcal{N}_r$. In practice, we want to have that $N_r \ll N_a$ so that the QC system (2.4) is much smaller than the molecular statics system (1.7). However, even though the system (2.4) has fewer degrees of freedom, the work involved in determining its solution still depends on N, the total number of particles. This is because in the assembly of the jth equation, the outer sum is over the particles located in the support of the basis function $\psi_j^h(\cdot)$, so that collectively the number of summands that have to be evaluated in the system (2.4) is of the order of N. In addition, each summand itself is a function of N variables so that the work in evaluating each summand also depends on N.

On the other hand, even if the approximate positions $\{\mathbf{x}_j^h\}_{j\in\mathcal{N}_r}$ of the representative particles are known, the evaluation of the approximate energy in (2.2) still requires work of complexity $O(N^2)$ because $\Phi(\{\mathbf{x}_\alpha^h\}_{\alpha\in\mathcal{N}})$ is a function of the positions of all particles.

3. Quadrature-rule (QC–QR) type approximation

Provided $N_r \ll N_a$, the application of the quasicontinuum (QC) method effectively reduces the degrees of freedom from N_a to N_r. However, it still involves the positions of all particles so that the complexity of the QC method depends on the total number of particles N. In this section, we introduce a quadrature-rule (QC–QR) type method to reduce the complexity of the QC method.

3.1. Quadrature rules

In the QC method, the dependence of the total number of particles is caused by both the outer and inner sums in (2.2) and (2.4) that directly or collectively involve the calculation of the positions of all particles. Thus to reduce the cost of the QC method, we start by considering these summations. In particular, there are three types of sums in the QC formulations (2.2) and (2.4), i.e., outer sums of the form

$$G = \sum_{\alpha\in\mathcal{N}} g(\mathbf{X}_\alpha) \quad \text{and} \quad G_j = \sum\nolimits_{\alpha\in\mathcal{N}_j} g(\mathbf{X}_\alpha) \quad \text{for } j\in\mathcal{N}_r \tag{3.1}$$

and inner sums

$$S_\alpha = \sum_{\beta\in\mathcal{N},\beta\neq\alpha} s(\mathbf{X}_\alpha,\mathbf{X}_\beta) \quad \text{for } \alpha\in\mathcal{N}, \tag{3.2}$$

where $g(\cdot)$ and $s(\cdot,\cdot)$ are appropriate functions. The basic idea of the QC–QR method is to:

1. break up the sums in (3.1) and (3.2) into sums over the representative particles $\mathbf{X}_j, j\in\widetilde{\mathcal{N}}_r$ and over the simplices $\Delta_t, t=1,\ldots,T$;
2. approximate the sum over the particles within an individual simplex Δ_t by a weighted sum over only a subset of those particles.

Let $\mathcal{N}_t = \{\alpha\in\mathcal{N}/\widetilde{\mathcal{N}}_r | \ \mathbf{X}_\alpha\in\overline{\Delta}_t\}$ denote the index set of the particles located inside or on the boundary of the simplex Δ_t that are not representative particles, i.e., not located at the vertices. Because all particles with positions specified by (1.1) have been chosen as representative particles, the position of any particle whose index belongs to $\mathcal{N}_t$ is not specified, i.e., $\mathcal{N}_t\subset\mathcal{N}_a$, for $t=1,2,\ldots,T$. If a particle is on the boundary between simplices but not at a vertex, it can be arbitrarily assigned to one of the simplices. Then the sums in (3.1) and (3.2) can be expressed in the form

$$\begin{aligned} G &= \sum_{t=1}^{T}\sum_{\alpha\in\mathcal{N}_t} g(\mathbf{X}_\alpha) + \sum_{k\in\widetilde{N}_r} g(\mathbf{X}_k), \\ G_j &= \sum_{t\in\mathcal{T}_j}\sum_{\alpha\in\mathcal{N}_t} g(\mathbf{X}_\alpha) + g(\mathbf{X}_j), \end{aligned} \tag{3.3}$$

and

$$S_\alpha = \sum_{t=1}^{T}\sum_{\beta\in\mathcal{N}_t,\beta\neq\alpha} s(\mathbf{X}_\alpha,\mathbf{X}_\beta) + \sum_{k\in\widetilde{\mathcal{N}}_r,k\neq\alpha} s(\mathbf{X}_\alpha,\mathbf{X}_k) \quad \text{for } \alpha\in\mathcal{N}. \tag{3.4}$$

In the following, we focus on the inner sums in (3.3) and (3.4). For each simplex Δ_t, we choose a subset

$$\mathcal{N}_{t,q} = \begin{cases} \mathcal{N}_t & \text{if } N_t\leqslant q \\ \text{a } q\text{-dimensional subset of } \mathcal{N}_t & \text{otherwise,} \end{cases} \tag{3.5}$$

i.e., in the latter case, $\mathcal{N}_{t,q}$ consists of q particles chosen from among the particles in the simplex Δ_t, where q depends on the "quadrature" rule we use. Then the sum over the particles within the simplex Δ_t can be approximated by a weighted sum over the subset of particles whose indices belong to $\mathcal{N}_{t,q}$, i.e., we have

$$\sum_{\alpha\in\mathcal{N}_t} g(\mathbf{X}_\alpha) \approx \sum_{\beta\in\mathcal{N}_{t,q}} \omega_{t,\beta} g(\mathbf{X}_\beta), \tag{3.6}$$

and

$$\sum_{\beta\in\mathcal{N}_t} s(\mathbf{X}_\alpha,\mathbf{X}_\beta) \approx \sum_{\beta\in\mathcal{N}_{t,q}} \omega_{t,\beta} s(\mathbf{X}_\alpha,\mathbf{X}_\beta), \tag{3.7}$$

where $\mathbf{X}_\beta$ is the "quadrature" particle chosen in the simplex Δ_t and $\omega_{t,\beta}$ denotes the corresponding "quadrature" weight. Roughly speaking, the weight $\omega_{t,\beta}$ can be viewed as the number of particles the quadrature particle $\mathbf{X}_\beta$ represents in the simplex Δ_t and is not necessarily an integer. In particular, when $N_t\leqslant q$, since all particles in the simplex Δ_t are chosen as the quadrature[4] particles, we have

[4] In the sequel, we drop putting the adjective quadrature within quotation marks but always keep in mind that, for us, quadrature particles are not true quadrature points.

$\omega_{t,\beta} \equiv 1$ and the sums (3.6) and (3.7) are exact for any function $g(\cdot)$ and $s(\cdot,\cdot)$.

When $N_t > q$, the basic requirement of selecting the quadrature particles $\{\mathbf{X}_\beta : \beta \in \mathscr{N}_{t,q}\}$ is that they are in general position.[5] This requirement is necessary for the linear system defining the weights to be invertible. The selection of the quadrature particle $\mathbf{X}_\beta$ and the computation of its weight $\omega_{t,\beta}$ are done in the reference configuration and thus are independent of the deformed positions of the particles. In addition, the same quadrature particles and weights can be used for all the steps of an iterative solution process for the equilibrium position of the particles. Details about the selection of $\mathbf{X}_\beta$ and the computation of $\omega_{t,\beta}$ are addressed in [19]; we only mention that the selection is made so that the approximate sums in, e.g., (3.6) and (3.7), agree with the exact sums for polynomials of a chosen degree.

3.2. The reduced equations of the QC–QR method

The function $g(\cdot)$ appearing in the summations G and G_j depends only on the position of the particles so we can directly apply the approximation (3.6) to the inner sums in (3.3) and obtain

$$G \approx \sum_{t=1}^{T} \sum_{\beta \in \mathscr{N}_{t,q}} \omega_{t,\beta} g(\mathbf{X}_\beta) + \sum_{k \in \widetilde{N}_r} g(\mathbf{X}_k), \tag{3.8}$$

$$G_j \approx \sum_{t \in \mathscr{T}_j} \sum_{\beta \in \mathscr{N}_{t,q}} \omega_{t,\beta} g(\mathbf{X}_\beta) + g(\mathbf{X}_j) \quad \text{for } j \in \mathscr{N}_r. \tag{3.9}$$

Consequently, the complexity in evaluating the sum G reduces from $O(N)$ in (3.1) to $O(qT + \widetilde{N}_r)$ in (3.8), where the number $qT + \widetilde{N}_r$ depends on the number of representative particles, the construction of the triangulation, and the quadrature rule used, but is independent of the total number of particles N. Similarly, the work involved in calculating G_j becomes independent of N_j. For instance, in the one-dimensional case, the complexity of (3.8) is of $O((q+1)\widetilde{N}_r)$ which is much smaller than the total number of particles N provided that $\widetilde{N}_r \ll N$. In addition, the complexity of (3.9) is of $O(2q+1)$, which is a constant depending only on the number of quadrature particles used in a simplex.

On the other hand, the function $s(\cdot,\cdot)$ depends not only on the position of the particle we consider but on its distance to the other particles. Thus we cannot simply apply the approximation (3.7) to all the simplices in (3.4), i.e., we have to take the distance between particles into account when approximating the sum (3.4). Thus, in the following, we divide our discussions for two cases: *short-range* and *long-range* interactions.

If the interaction between particles is short-range, i.e., the magnitude of the interaction potential decays very fast with respect to the distance of two particles, we can neglect the interaction over large distances and truncate the potential energy into a small region. Thus, we assume that [26]

$$|\Phi^a_{\alpha,\beta}(\mathbf{x}_\alpha, \mathbf{x}_\beta)| = 0 \quad \text{when } |\mathbf{x}_\alpha - \mathbf{x}_\beta| > r_c, \tag{3.10}$$

where $r_c > 0$ is the truncation radius of the potential energy, i.e., we assume that there is no interaction between two particles whose distance is larger than r_c units. Let

$$\mathscr{N}_{b(\alpha)} = \{\beta \in \mathscr{N} | 0 < |\mathbf{x}_\alpha - \mathbf{x}_\beta| \leqslant r_c\} \tag{3.11}$$

denote the index set of particles whose distance from particle α is not larger than r_c. Then the sum in (3.2) reduces to

$$S_\alpha \approx \sum_{\beta \in \mathscr{N}_{b(\alpha)}} s(\mathbf{X}_\alpha, \mathbf{X}_\beta) \quad \text{for } \alpha \in \mathscr{N}. \tag{3.12}$$

[5] A set of points in $\mathbb{R}^d$ is said to be in general position if no $d+1$ of them lie in a $(d-1)$-dimensional hyperplane.

Thus, for any particle $\alpha \in \mathscr{N}$, we only consider its interaction with those particles located within its neighboring region and apply the full atomistic resolution in that region. It is easy to see that, in this case, the complexity of S_α in (3.2) reduces to $O(N_{b(\alpha)})$ which is independent of the total number of particles N; see [19] for a detailed discussion.

On the other hand, if the interaction between particles is long-ranged, the interaction potential decays slowly and cannot be ignored even though the distance between two particles is large [20]. In this case, we apply the full atomistic resolution in a close-in region of particle α but, for the far-away region, the quadrature-rule type approximation is applied. To do this, we denote by

$$\mathscr{T}_{\alpha,r} = \{t \in \{1,\dots,T\} | \operatorname{dist}(\mathbf{X}_\alpha, \overline{\Delta}_t) \leqslant r_c\} \quad \text{for } \alpha \in \mathscr{N} \tag{3.13}$$

the index set of simplices whose distance from particle α is not larger than r_c units. The distance between the particle α and a simplex Δ_t is defined by

$$\operatorname{dist}(\mathbf{X}_\alpha, \overline{\Delta}_t) = \max_{\beta \in \mathscr{N}_t} |\mathbf{X}_\beta - \mathbf{X}_\alpha|.$$

Then in the case of long-range interactions, the summation in (3.2) can be approximated by

$$\begin{aligned} S_\alpha &= \sum_{\beta \in \mathscr{N}_{b(\alpha)}} s(\mathbf{X}_\alpha, \mathbf{X}_\beta) + \sum_{\beta \notin \mathscr{N}_{b(\alpha)}} s(\mathbf{X}_\alpha, \mathbf{X}_\beta) \\ &\approx \sum_{\beta \in \mathscr{N}_{b(\alpha)}} s(\mathbf{X}_\alpha, \mathbf{X}_\beta) + \sum_{t \notin \mathscr{T}_{\alpha,r}} \sum_{\beta \in \mathscr{N}_{t,q}} \omega_{t,\beta} s(\mathbf{X}_\alpha, \mathbf{X}_\beta) + \sum_{k \in \widetilde{\mathscr{N}}_r, k \neq \alpha} s(\mathbf{X}_\alpha, \mathbf{X}_k), \end{aligned} \tag{3.14}$$

where the index set $\mathscr{N}_{b(\alpha)}$ is defined in (3.11). Consequently, the complexity in evaluating the summation S_α in (3.14) is bounded by the number $N_{b(\alpha)} + qT + \widetilde{N}_r$, which is independent of the total number of particles N provided that the number $N_{b(\alpha)} \ll N$ and $\widetilde{N}_r \ll N$.

In fact, we can rewrite the approximation of S_α for the short-range interactions in (3.12) and for the long-range interactions in (3.14) in a uniform way, i.e.,

$$S_\alpha \approx \sum_{\beta \in \mathscr{N}_{b(\alpha)}} s(\mathbf{X}_\alpha, \mathbf{X}_\beta) + \sum_{t \notin \mathscr{T}_{\alpha,r}} \sum_{\beta \in \mathscr{N}_{t,q}} \omega_{t,\beta} s(\mathbf{X}_\alpha, \mathbf{X}_\beta) + \sum_{k \in \widetilde{\mathscr{N}}_r, k \neq \alpha} \omega_k s(\mathbf{X}_\alpha, \mathbf{X}_k), \tag{3.15}$$

where

$$\begin{cases} \omega_k \equiv 0 \quad \text{and} \quad \omega_{t,\beta} \equiv 0, & \text{for short-range interactions} \\ \omega_k \equiv 1, & \text{for long-range interactions.} \end{cases}$$

By applying (3.8) and (3.15), respectively, to the outer and inner summations appearing in the total potential energy (2.2), we obtain the *energy-based QC–QR method*, i.e.,

$$\begin{aligned} &\Phi^h(\{\mathbf{x}^h_k\}_{k \in \widetilde{\mathscr{N}}_r}) \\ &\approx \sum_{\tau=1}^{T} \sum_{\alpha \in \mathscr{N}_{\tau,p}} \omega_{\tau,\alpha} \left(\sum_{\beta \in \mathscr{N}_{b(\alpha)}} \frac{\Phi^a_{\alpha,\beta}(\mathbf{x}^h_\alpha, \mathbf{x}^h_\beta)}{2} + \sum_{k \in \widetilde{\mathscr{N}}_r} \omega_k \frac{\Phi^a_{\alpha,k}(\mathbf{x}^h_\alpha, \mathbf{x}^h_k)}{2} \right. \\ &\quad \left. + \sum_{t \notin \mathscr{T}_{\alpha,r}} \sum_{\beta \in \mathscr{N}_{t,q}} \omega_{t,\beta} \frac{\Phi^a_{\alpha,\beta}(\mathbf{x}^h_\alpha, \mathbf{x}^h_\beta)}{2} + \Phi^e_\alpha(\mathbf{x}^h_\alpha) \right) \\ &\quad + \sum_{j \in \widetilde{\mathscr{N}}_r} \left(\sum_{\beta \in \mathscr{N}_{b(j)}} \frac{\Phi^a_{j,\beta}(\mathbf{x}^h_j, \mathbf{x}^h_\beta)}{2} + \sum_{k \in \widetilde{\mathscr{N}}_r, k \neq j} \omega_k \frac{\Phi^a_{j,k}(\mathbf{x}^h_j, \mathbf{x}^h_k)}{2} \right. \\ &\quad \left. + \sum_{t \notin \mathscr{T}_{j,r}} \sum_{\beta \in \mathscr{N}_{t,q}} \omega_{t,\beta} \frac{\Phi^a_{j,\beta}(\mathbf{x}^h_j, \mathbf{x}^h_\beta)}{2} + \Phi^e_j(\mathbf{x}^h_j) \right) \end{aligned} \tag{3.16}$$

subject to (1.1) and (2.1). In the approximation (3.16), we use $p > 0$ and $q > 0$ quadrature particles for the outer and inner summations, respectively. Note that it is not necessary to require that $p = q$ even on the same simplex Δ_t, i.e., we may use different quadrature rules for the sums in (3.1) and (3.2).

Similarly, to determine the degrees of freedom, one can differentiate the approximate energy in (3.16) with respect to the position $\mathbf{x}_i^h$, for $i \in \mathcal{N}_r$, and solve the resulting force equilibrium equations. Alternatively, in practice we can work with the *force-based QC–QR method*. It is obtained by applying the approximations (3.9) and (3.15) to the equations in (2.4), i.e., for $j \in \mathcal{N}_r$,

$$\begin{cases} \sum_{\tau\in\mathcal{T}_j} \sum_{\alpha\in\mathcal{N}_{\tau,p}} \omega_{\tau,\alpha}\psi_j^h(\mathbf{X}_\alpha)\left(\sum_{\beta\in\mathcal{N}_{b(\alpha)}} \mathbf{f}^a_{\alpha,\beta}(\mathbf{x}_\alpha^h,\mathbf{x}_\beta^h)\right. \\ \left. + \sum_{t\notin\mathcal{T}_{\alpha,r}} \sum_{\beta\in\mathcal{N}_{t,q}} \omega_{t,\beta}\mathbf{f}^a_{\alpha,\beta}(\mathbf{x}_\alpha^h,\mathbf{x}_\beta^h) + \sum_{k\in\mathcal{N}_r} \omega_k \mathbf{f}^a_{\alpha,k}(\mathbf{x}_\alpha^h,\mathbf{x}_k^h) + \mathbf{f}^e_\alpha(\mathbf{x}_\alpha^h)\right) \\ + \left(\sum_{\beta\in\mathcal{N}_{b(j)}} \mathbf{f}^a_{j,\beta}(\mathbf{x}_j^h,\mathbf{x}_\beta^h) + \sum_{k\in\mathcal{N}_r,k\neq j} \omega_k \mathbf{f}^a_{j,k}(\mathbf{x}_j^h,\mathbf{x}_k^h)\right. \\ \left. + \sum_{t\notin\mathcal{T}_{j,r}} \sum_{\beta\in\mathcal{N}_{t,q}} \omega_{t,\beta}\mathbf{f}^a_{j,\beta}(\mathbf{x}_j^h,\mathbf{x}_\beta^h) + \mathbf{f}^e_j(\mathbf{x}_j^h)\right) = \mathbf{0}, \\ \text{where } \mathbf{x}_\alpha^h = \mathbf{x}_\alpha^0 \quad \text{if } \alpha\in\mathcal{N}_f; \quad \mathbf{x}_\alpha^h = \sum_{k\in\mathcal{N}_r} \mathbf{x}_k^h\psi_k^h(\mathbf{X}_\alpha) \quad \text{if } \alpha\in\mathcal{N}_a. \end{cases} \tag{3.17}$$

Our numerical simulations suggest that, using the same iterative solution method, the system (3.17) can yield the same solution as that from the system obtained by explicitly differentiating (3.16). However, using (3.17) requires substantially lower computational time. Thus, in the following, we always refer to the system (3.17) as the force equilibrium equations of the QC–QR method.

4. Error analysis

In this section, we analyze the accuracy and complexity of the QC–QR method by using a simple one-dimensional (1D) monoatomic chain with N particles so that we have the index set $\mathcal{N} = \{1,\dots,N\}$. In the reference configuration, all particles are uniformly distributed on a straight line with an interparticle distance h. For simplicity, we choose $h = 1$ and define the position of the particle α by $X_\alpha = \alpha h = \alpha$ for $\alpha \in \mathcal{N}$. A triangulation $\mathsf{T}_h = \{\Delta_t\}_{t=1}^{N_r-1}$ is constructed with the uniform simplex size $L = (N-1)/(\tilde{N}_r - 1) > 0$, where $\tilde{N}_r$ is the number of the representative particles. Then the coordinate of the representative particle j is denoted by $\tilde{X}_j = (j-1)L + 1$ for $j = 1,\dots,\tilde{N}_r$ and the simplices are $\Delta_t = (\tilde{X}_j, \tilde{X}_{j+1})$ for $t = j = 1,\dots,\tilde{N}_r - 1$. In the following, we assume that the simplex size $L \gg 1$ so that $\tilde{N}_r \ll N$.

To analyze the accuracy the QC–QR method, especially in the long-range interaction case, we choose the interaction potential as

$$\Phi^a_{\alpha,\beta}(X_\alpha, X_\beta) = \frac{\kappa}{|X_\alpha - X_\beta|} \quad \text{with } \kappa \text{ a constant}, \tag{4.1}$$

and assume that $\Phi^e_\alpha(X) = 0$ for $\alpha \in \mathcal{N}$, i.e., no external potential is applied on the chain. On each simplex Δ_t, two quadrature particles are used, and they are chosen to be on the Gaussian quadrature points of this simplex, i.e.,

$$X_{t,\beta} = X_j + \left(\frac{1}{2} \pm \frac{\sqrt{3}}{6}\right)L \quad \text{for } \beta = 1,2. \tag{4.2}$$

Here, we assume that there exist particles exactly at these two points. In practice, if this is not the case, one can choose the particles that are nearest to these quadrature points. Then the weights of $X_{t,\beta}$ can be calculated as

$$\omega_{t,1} = \omega_{t,2} := \omega = \frac{L-1}{2}, \tag{4.3}$$

i.e., each quadrature particle represents $(L-1)/2$ particles within the simplex Δ_t. Unless otherwise stated, we will always use two quadrature particles for both the outer and inner summations, i.e., we set $p = q = 2$ in (3.16).

If we view the representative particles as simplices having only one particle, then the interactions in the first term of the energy (2.2) can be broken into the interactions between simplices. Thus, without loss of generality, we consider the interaction between two simplices Δ_{t_1} and Δ_{t_2} (see Fig. 1) and calculate the total potential energy S due to the interaction between particles $X_\alpha \in \Delta_{t_1}$ and $X_\beta \in \Delta_{t_2}$. In this case, the QC method always gives the exact interaction potential energy, i.e., $S_{\text{exact}} = S_{\text{QC}}$. We assume that $t_2 \geqslant t_1$ and $l = t_2 - (t_1 + L)$; see Fig. 1.

Then divide our discussion into the following three cases.

Case 1. $l > 0$, i.e., Δ_{t_1} and Δ_{t_2} are not neighboring simplices. In this case, the energy by the QC method is

$$\begin{aligned} S_{\text{QC}} &= \sum_{\alpha=t_1+1}^{t_1+L-1} \sum_{\beta=t_2+1}^{t_2+L-1} \Phi^a_{\alpha,\beta}(X_\alpha, X_\beta) = \kappa \sum_{i=1}^{L-1} \sum_{r=L+l+1-i}^{2L+l-1-i} \frac{1}{r} \\ &= \kappa\left[\frac{L-1}{l+L} + (l+2L-1)\sum_{r=l+L+1}^{l+2L-2}\frac{1}{r} - (l+1)\sum_{r=l+2}^{l+L-1}\frac{1}{r}\right]. \end{aligned} \tag{4.4}$$

Assume that $l = aL$ with $a \geqslant 1$ an integer. Then noting that $L \gg 1$, we have

$$\begin{aligned} S_{\text{QC}} &\approx \kappa\left[\frac{L-1}{l+L} + (l+2L-1)\left(\ln\frac{l+2L-2}{l+L} - \frac{L-2}{2(l+L)(l+2L-2)}\right)\right. \\ &\quad \left. -(l+1)\left(\ln\frac{l+L-1}{l+1} - \frac{L-2}{2(l+1)(l+L-1)}\right)\right] \\ &\approx \kappa\left[L\left(a\ln\frac{(a+2)a}{(a+1)^2} + 2\ln\frac{(a+2)}{(a+1)}\right) + \frac{1}{a+1}\right]. \end{aligned}$$

It is easy to obtain the leading order of S_{QC} as

$$S_{\text{QC}} \sim \kappa L\left(a\ln\frac{(a+2)a}{(a+1)^2} + 2\ln\frac{(a+2)}{(a+1)}\right) \quad \text{when } L \gg 1. \tag{4.5}$$

On the other hand, the QC–QR method gives that

$$\begin{aligned} S_{\text{QC–QR}} &= \sum_{\alpha=1}^{2}\omega_{t_1,\alpha}\sum_{\beta=1}^{2}\omega_{t_2,\beta}\Phi^a_{\alpha,\beta}(X_{t_1,\alpha}, X_{t_2,\beta}) \\ &= \omega^2\sum_{\alpha=1}^{2}\sum_{\beta=1}^{2}\Phi^a_{\alpha,\beta}(X_{t_1,\alpha}, X_{t_2,\beta}) \\ &= \kappa\left(\frac{L-1}{2}\right)^2\left[\frac{2}{l+L} + \frac{1}{l+(1+\sqrt{3}/3)L} + \frac{1}{l+(1-\sqrt{3}/3)L}\right]. \end{aligned}$$

Similarly, when $L \gg 1$ and $a \geqslant 1$, the leading order of $S_{\text{QC–QR}}$ is

$$\begin{aligned} S_{\text{QC–QR}} &\sim \kappa L\frac{(a+1)^2 - 1/6}{(a+1)(a+1-\sqrt{3}/3)(a+1+\sqrt{3}/3)} \\ &\approx \kappa L\frac{a+1}{(a+1-\sqrt{3}/3)(a+1+\sqrt{3}/3)}. \end{aligned} \tag{4.6}$$

To compare S_{QC} and $S_{\text{QC–QR}}$, we define the relative error

$$e_{\text{QC–QR}} = \left|\frac{S_{\text{QC–QR}} - S_{\text{QC}}}{S_{\text{QC}}}\right| = \left|\frac{S_{\text{QC–QR}} - S_{\text{exact}}}{S_{\text{exact}}}\right|. \tag{4.7}$$

For a fixed simplex size $L = 500$, Fig. 2 shows the results $S_{\text{QC}}, S_{\text{QC–QR}}$ and $e_{\text{QC–QR}}$ for different simplex distance l. We see that the relative error $e_{\text{QC–QR}}$ decreases very fast when the distance between two simplices increases. Thus when the distance l becomes sufficiently

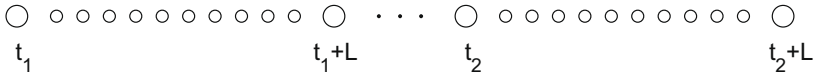

Fig. 1. Two simplices Δ_{t_1} and Δ_{t_2} in the 1D monoatomic chain with $L = 11$, where the "big" particles are the representative particles.

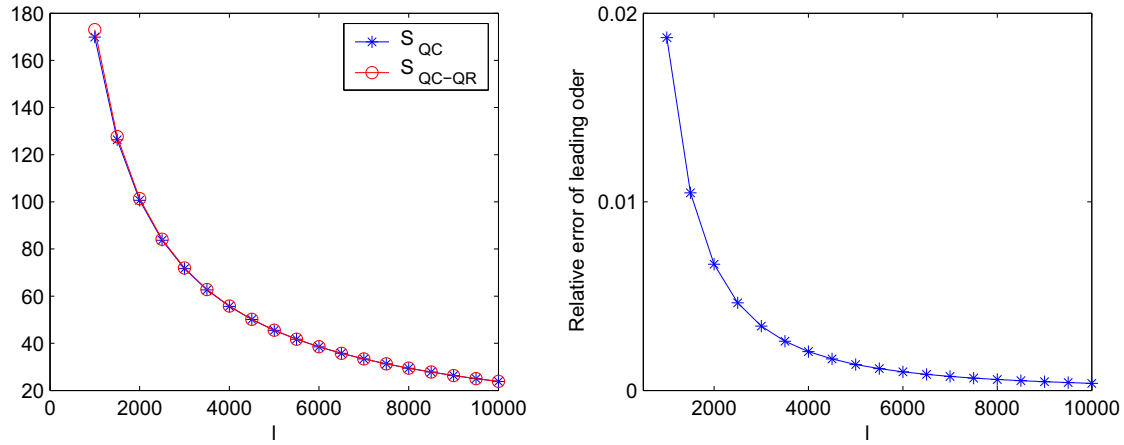

Fig. 2. The approximate energies S_{QC} and S_{QC-QR} (left) and the relative error e_{QC-QR} (right) for different simplex distance l, where the simplex size is fixed at $L = 500$.

large, the error of S_{QC-QR} can be neglected and the QC–QR method provides a good approximation. On the other hand, Fig. 2 (left) shows that even though the distance l is large, the interaction potential between two simplices is not negligible. For example, when the distance $l = 10^4$, the interaction potential $S > 20$, which is still significant compared to $S = 1600$ when $l = 0$. This again suggests that in the case of long-range interactions, the interactions from far-away regions cannot be ignored.

Case 2. $l = 0$, i.e., Δ_{t_1} and Δ_{t_2} are two neighboring simplices. Substituting $l = 0$ into (4.4), we obtain

$$\begin{aligned} S_{QC} &= \kappa\left(\frac{L-1}{L} + (2L-1)\sum_{r=L+1}^{2L-2}\frac{1}{r} - \sum_{r=2}^{L-1}\frac{1}{r}\right) \\ &\approx \kappa\left[\frac{L-1}{L} + (2L-1)\left(\ln\frac{2(L-1)}{L} - \frac{L-2}{4L(L-1)}\right)\right. \\ &\quad \left. -\left(\ln(L-1) - (1-\gamma) + \frac{1}{2(L-1)}\right)\right], \end{aligned}$$

where $\gamma \approx 0.5772$ is the Euler–Mascheroni number. When $L \gg 1$, the leading order of S_{QC} is

$$S_{QC} \sim 2\kappa L \ln\frac{2(L-1)}{L} \sim \kappa L \ln 4. \tag{4.8}$$

Similarly, when $l = 0$, we have

$$S_{QC-QR} = \kappa\left(\frac{L-1}{2}\right)^2\left[\frac{2}{L} + \frac{1}{(1+\sqrt{3}/3)L} + \frac{1}{(1-\sqrt{3}/3)L}\right],$$

which implies the leading order

$$S_{QC-QR} \sim \frac{5}{4}\kappa L \quad \text{as } L \gg 1. \tag{4.9}$$

When $L \gg 1$, the relative error between (4.8) and (4.9) is $e_{QC-QR} \approx 0.098$. In the above calculation, we use two-point quadrature rule for both the inner and outer sums, i.e., $p = q = 2$ in (3.16). In practice, to improve the accuracy of the QC–QR method, one may use higher order quadrature rules, i.e., choosing $p, q > 2$. For example, when $L \gg 1$, if we fix $p = 2$, then

$$\begin{aligned} S_{QC-QR} &\sim 1.28\kappa L \quad \text{and} \quad e_{QC-QR} \approx 0.078, \quad \text{if } q = 3, \\ S_{QC-QR} &\sim 1.30\kappa L \quad \text{and} \quad e_{QC-QR} \approx 0.062, \quad \text{if } q = 5. \end{aligned}$$

Fig. 3 presents more results for different q and simplex size L, where $p = 2$ is fixed in (3.16). It shows that for a fixed simplex size L, the more quadrature particles one uses, the smaller the error. On the other hand, for a fixed number of quadrature particles q, when the simplex size L is large enough, the error e_{QC-QR} becomes almost a constant which is independent of L. In this case, we consider a typical simplex distance $l = 0$. In fact, for any l, using more quadrature particles can always lead to a better approximation.

In addition, in the above two cases, i.e., $l > 0$ and $l = 0$, the computational complexity of the QC–QR method is of the order of pq. It is independent of the simplex size L and much smaller than the complexity of the QC method, which is $O(L^2)$, especially when L is very large.

Case 3. $l < 0$, i.e., $\Delta_{t_1} = \Delta_{t_2} := \Delta_t$ are the same simplices. In this case, we have

$$\begin{aligned} S_{QC} &= \sum_{\alpha=t+1}^{t+L-2}\sum_{\beta=\alpha+1}^{t+L-1}\Phi^a_{\alpha,\beta}(X_\alpha, X_\beta) = \kappa\sum_{i=1}^{L-2}\sum_{r=1}^{L-1-i}\frac{1}{r} \\ &= \kappa\left[(L-1)\sum_{r=1}^{L-2}\frac{1}{r} - (L-2)\right] \\ &\approx \kappa\left[(L-1)\left(\ln(L-2) + \gamma + \frac{1}{2(L-2)}\right) - (L-2)\right]. \end{aligned}$$

When $L \gg 1$, the leading order of S_{QC} is

$$S_{QC} \sim \kappa L(\ln(L-2) - (1-\gamma)). \tag{4.10}$$

In this case, the QC–QR method gives that

$$\begin{aligned} S_{QC-QR} &= \sum_{\alpha=1}^{2}\omega_{t,\alpha}\left(\sum_{\beta\in(\mathcal{N}_{b(\alpha)}\cap\mathcal{N}_t)}\frac{\Phi^a_{\alpha,\beta}(X_\alpha,X_\beta)}{2} + \sum_{\beta=1,\beta\neq\alpha}^{2}\omega'_{t,\beta}\frac{\Phi^a_{\alpha,\beta}(X_\alpha,X_\beta)}{2}\right) \\ &= \kappa\left(\frac{L-1}{2}\right)\left[2\sum_{\beta\in\mathcal{N}_t, 0<|\beta-\alpha|\leqslant r_c}\frac{1}{2|X_\beta - X_\alpha|} + 2\omega'_{t,\beta}\frac{1}{2\sqrt{3}L/3}\right], \end{aligned}$$

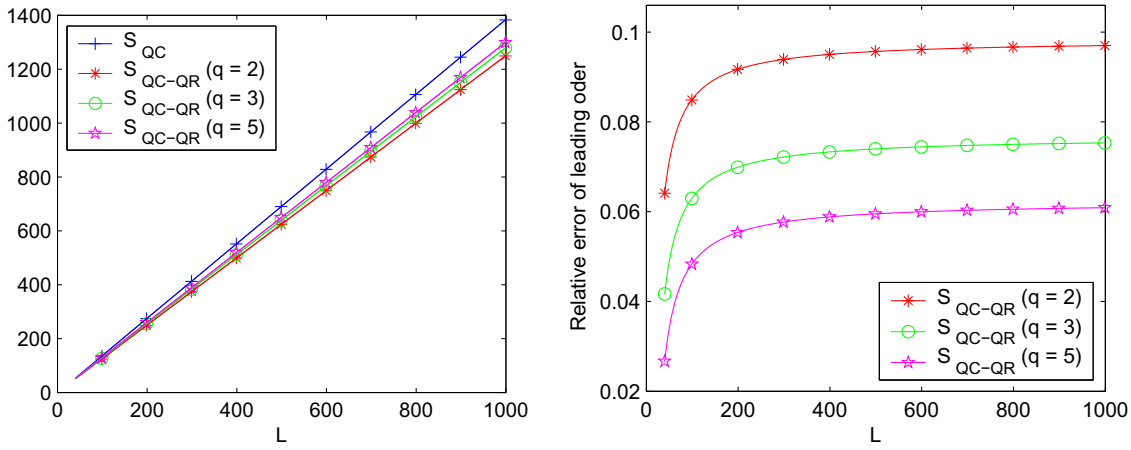

Fig. 3. The approximate energies S_{QC} and S_{QC-QR} (left) and the relative errors e_{QC-QR} (right) for different simplex size L and different numbers of quadrature particles q, where $p = 2$ is fixed in (3.16).

where the weight $\omega'_{t,\beta}$ is the number of particles the quadrature particle $\mathbf{X}_\beta$ represents, which are located inside of the simplex but their indices do not belong to $\mathcal{N}_{b(\alpha)}$. We can simply let

$$\omega'_{t,\beta} = \begin{cases} L - 1 - 2r_c & \text{if } 2r_c < L - 1 \\ 0 & \text{otherwise.} \end{cases}$$

As already mentioned, our motivation is to eliminate the dependence of the calculation on the total number of particles N. Thus only the case with $r_c \ll L$ is of interest. Assuming that $r_c \ll L$, we have, to the leading order,

$$S_{QC-QR} \sim \kappa L \left(\sum_{r=1}^{r_c} \frac{1}{r} + \frac{\sqrt{3}}{2} \right), \quad \text{for } L \gg 1 \quad \text{and} \quad r_c \ll L. \tag{4.11}$$

Fig. 4 shows the results for S_{QC}, S_{QC-QR}, and e_{QC-QR} for different simplex size L and different values of the radius r_c used in the QC–QR method. We see that for a fixed simplex size L, the accuracy of the QC–QR method can be greatly increased by using a larger radius size r_c. On the other hand, the computational cost of the QC–QR method is of the order $O(4(r_c + 1))$ which is much smaller than $O(L^2)$, the complexity of the QC method, provided that $L \gg 1$ and $r_c \ll L$.

5. Numerical tests

In this section, we computationally test the accuracy and efficiency of the quadrature-rule (QC–QR) type method by comparing it with the full atomistic method, the QC method and the cluster summation (QC–CS) method. Comparisons for short-range interaction problems between the QC–QR method and cluster summation methods such as that discussed in [12] were presented in [19]. Here, we do not include such comparisons because cluster summation methods in general become dependent on the total number of degrees of freedom (and not just on the number of representative particles) for long-range interaction problems.

A simple one-dimensional monoatomic chain with N particles is studied. The displacement and displacement gradient are defined by

$$\mathbf{u}(\mathbf{X}) = \mathbf{x} - \mathbf{X} \quad \text{and} \quad F(\mathbf{X}) = \frac{d\mathbf{x}}{d\mathbf{X}} = \mathbf{I} + \frac{d\mathbf{u}}{d\mathbf{X}}, \tag{5.1}$$

respectively, where $\mathbf{I}$ is the identity tensor, and $\mathbf{X}$ and $\mathbf{x}$ are the positions in the reference and a deformed configuration, respectively. To quantify the accuracy, we define the position error

$$e_{L^2}(\mathbf{x}) = \|\mathbf{x}_1 - \mathbf{x}_2\|_{L^2} = \frac{\sqrt{\sum (\mathbf{x}_1 - \mathbf{x}_2)^2}}{N}, \tag{5.2}$$

where $\mathbf{x}_1$ and $\mathbf{x}_2$ are the solutions obtained from the two different methods being compared. The relative error in the energy is defined by

$$e(\Phi) = \frac{|\Phi(\mathbf{x}) - \Phi^h(\mathbf{x}^h)|}{|\Phi(\mathbf{x})|}, \tag{5.3}$$

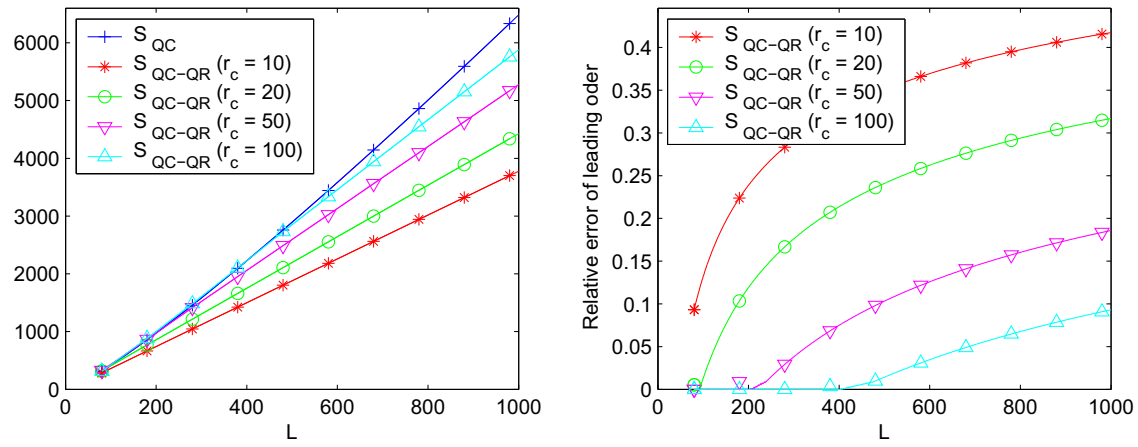

Fig. 4. The approximate energies S_{QC} and S_{QC-QR} (left) and the relative errors e_{QC-QR} (right) for different simplex size L and different radius r_c in the QC–QR method.

where $\mathbf{x}$ is the solution by the full atomistic method and $\mathbf{x}^h$ is that from the approximate methods, i.e., from the QC method or the QC–QR method.

In our examples, we use a pairwise interaction potential. For the case of short-range interactions, the 6–12 Lennard–Jones potential

$$\Phi^a_{\mathrm{LJ}}(r) = 4\epsilon_0\left(\left(\frac{\sigma}{r}\right)^{12} - 2\left(\frac{\sigma}{r}\right)^{6}\right) \quad \text{for } r = |\mathbf{x}_\alpha - \mathbf{x}_\beta| \tag{5.4}$$

is used [12,27] with ϵ_0 the parameter determining the depth of the potential well and σ the length scale determining the position at which the potential attains its minimum. In the case of long-range interactions, we use a simple combination of the Lennard–Jones potential in (5.4) and the Coulomb potential so that the interaction potential is given by

$$\Phi^a_{\alpha,\beta}(\mathbf{x}_\alpha, \mathbf{x}_\beta) := \Phi^a(r) = \Phi^a_{\mathrm{LJ}}(r) + \Phi^a_{\mathrm{C}}(r) \quad \text{with } r = |\mathbf{x}_\alpha - \mathbf{x}_\beta|, \tag{5.5}$$

where the Coulomb potential Φ^a_{C} takes the form

$$\Phi^a_{\mathrm{C}}(r) = \frac{1}{4\pi\epsilon_1}\frac{q_\alpha q_\beta}{r} \quad \text{for } r = |\mathbf{x}_\alpha - \mathbf{x}_\beta|. \tag{5.6}$$

The parameter ϵ_1 is the electrical permittivity of free space and q_α and q_β are the electric charges carried by particle α and β, respectively. Fig. 5 shows plots of the different interaction potentials defined in (5.4)–(5.6).

In addition, an external potential is applied to this monoatomic chain; it has the form

$$\Phi^e(\mathbf{x}) = A(R - \mathbf{x})^2, \tag{5.7}$$

where $A, R > 0$ are two constants.

In the simulations, we use $N = 4096$ particles and, in the reference configuration, all particles are uniformly distributed along a straight line with an interparticle distance $h = 1$. The two end-particles are fixed by requiring that $\mathbf{u}(\mathbf{X}_1) = \mathbf{u}(\mathbf{X}_{4096}) = 0$. The parameters in the potentials are chosen as $\epsilon_0 = 1$ and $\sigma = 1$ in (5.4), $\epsilon_1 = 0.01$ and $A = 0.01/N$ and $R = N/2$ in (5.7). The selection of the representative particles and definition of the simplices are the same as in Section 4. In the QC–QR method, on each simplex, at most two quadrature particles are used for both the outer and inner sums, i.e., we choose $p = q = 2$ in (3.16) and (3.17).

In the following plots, we use "FA" to denote results obtained from the full atomistic method, i.e., (1.5) and (1.7). Similarly, "QC" denote results from the QC method, i.e., (2.2) and (2.4) and "QC–QR" from the QC–QR method, i.e., (3.16) and (3.17).

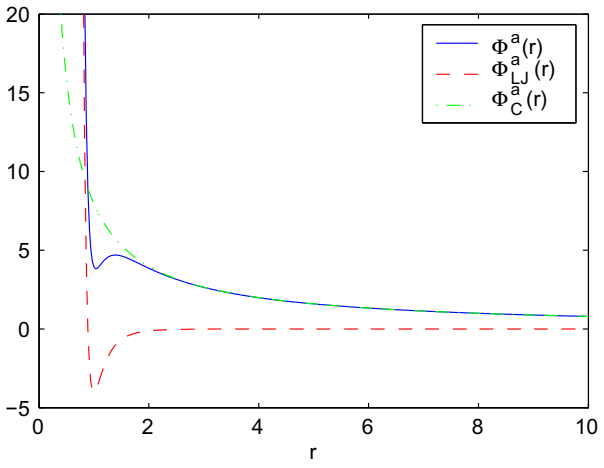

Fig. 5. The interaction potential as a function of the distance between two particles, with $\epsilon_0 = \sigma = 1$ in (5.4) and $\epsilon_1 = 0.01$ and $|q_\alpha| = |q_\beta| = 1$ in (5.5) and (5.6).

5.1. Example I. Short-range interactions

In this example, we consider short-range interatomic interactions, using the potential defined in (5.4). Fig. 6 shows the FA displacement $\mathbf{u}(\mathbf{X})$ and displacement gradient $\mathbf{F}(\mathbf{X})$ of the particle chain. We see that the deformation is highly nonuniform due to the external force.

To compare the QC–QR method with the QC method, we study cases with different numbers of representative particles and calculate the errors for both the positions and energy. For different number of representative particles, Fig. 7 plots the position error $e_{L^2}(\mathbf{x})$ of the QC and QC–QR methods and also the time consumed for solving the force equilibrium equations; Fig. 8 displays the similar results for the energy. To further compare, Fig. 9 shows the relation between the error and the computing time.

Compared with the full atomistic method, the errors of the QC and QC–QR methods both decrease when more representative particles are used. On the other hand, for the same number of representative particles, the error of the QC–QR type method is always larger than that of the QC method. This is because, for the QC method, the error only comes from the reduction of the number of degrees of freedom from N_a to N_r through the use of the Cauchy–Born rule and the use of representative particles whereas, for the QC–QR method, it also includes the additional error caused by using quadrature rules to approximate the sums in the QC method.

Fig. 7 (right) shows that the computational time of the QC method is almost a constant for different numbers of representative particles $\tilde{N}_r$. Especially, the time used by the QC method in evaluating the total energy is always the same for different $\tilde{N}_r$; see Fig. 8 (right). In contrast, the time by the QC–QR method decreases very quickly when fewer representative particles are used. Furthermore, Fig. 9 shows that, *to obtain the same error, the computational time required by the QC–QR method is much lower than that for the QC method*. This is due to the fact that the costs associated with the QC method are dominated by the summations over all particles whereas the costs for the QC–QR method are mainly determined by the number of representative particles. Thus the fewer the representative particles, the smaller the cost for the QC–QR method.

In addition, Fig. 10 shows the time used in solving the force equilibrium equations and in evaluating the energy for different number of particles N and representative particles $\tilde{N}_r$. For the QC method, we see the quadratic dependence of the time with respect to N, whereas for the QC–QR method we see that the time is relatively insensitive to the value of N.

5.2. Example II. Long-range interactions

In some settings, interactions between particles are usually composed of both the short-range and long-range types. Thus, in this example, we use the potential in (5.5) and assume that all particles carry positive unit charges, i.e., $q_\alpha = +1$ for $\alpha \in \mathcal{N}$. Fig. 11 plots the FA displacement and displacement gradient of all particles. Figs. 12 and 13 illustrate the errors and the computing time for the force equilibrium equations and the total energy, respectively, with repect to different number of representative particles. In addition, Fig. 14 shows the relation between the errors and the computing time used by the QC and QC–QR methods. Fig. 15 shows the time used in solving the force equilibrium equations and in evaluating the energy for different number of particles N and representative particles $\tilde{N}_r$. For the QC method, we see the quadratic dependence on N of the time used; this effect is so dominant that the number of representative particles hardly affects the time used. On the other hand, for the QC–QR method, we see that for a fixed number of representative particles, the time used is largely independent of the number of particles N and is generally much lower

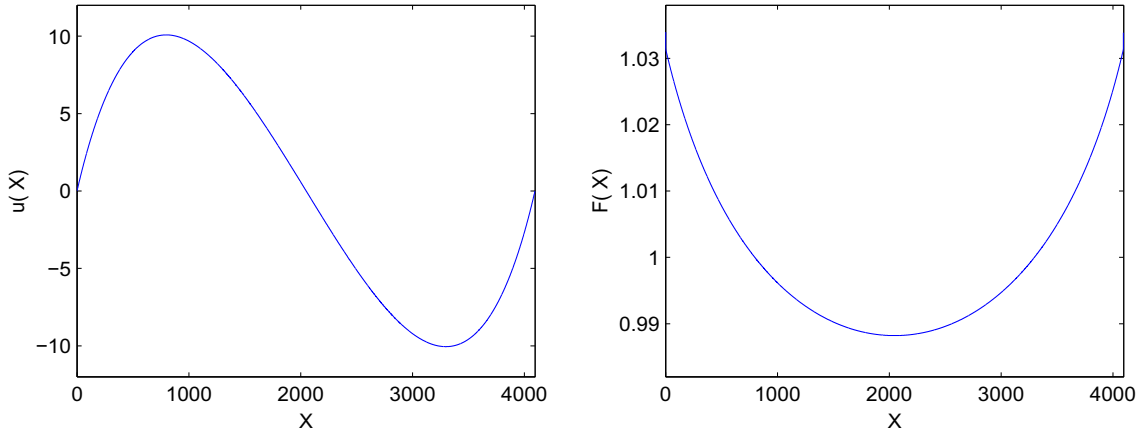

Fig. 6. Displacement (left) and displacement gradient (right) of the monoatomic chain in the short-range interaction case.

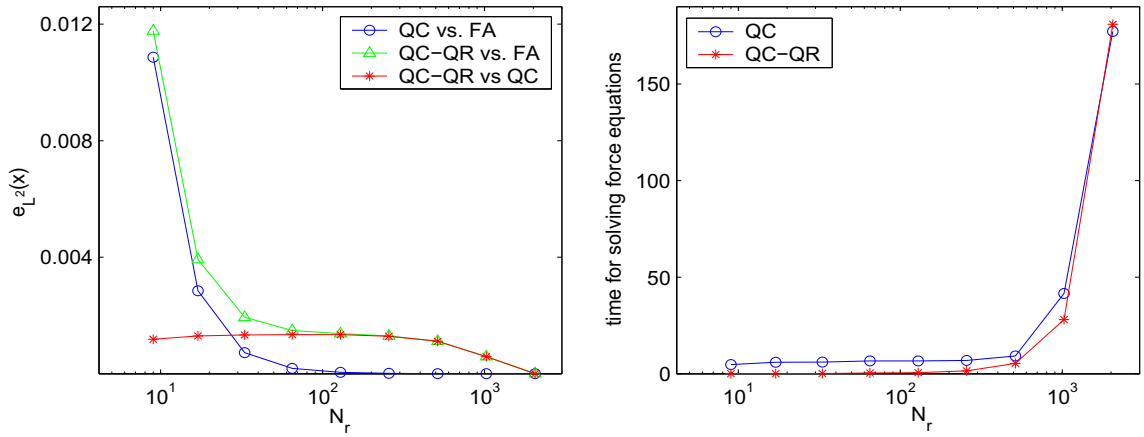

Fig. 7. Position errors (left) and the time used in solving the force equilibrium equations (right) for different numbers of representative particles in the short-range interaction case, where the total number of particles $N = 4096$.

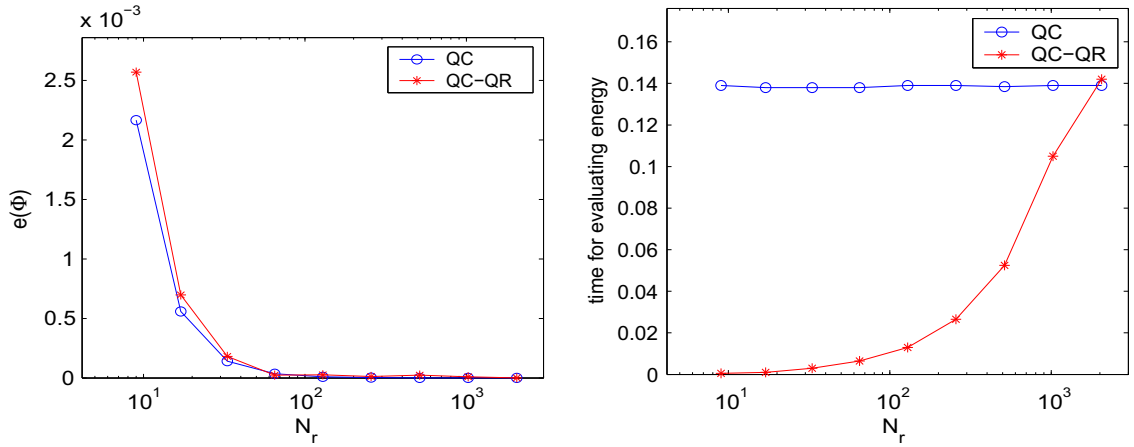

Fig. 8. Relative energy errors (left) and the time used in evaluating energy (right) for different numbers of representative particles in the short-range interaction case, where the total number of particles $N = 4096$.

than the time used in the QC method. We now do see a dependence on the number of representative particles as is expected because now the cost is no longer dominated by calculations that have complexity dependent on N. These results illustrate the important point *that the complexity of the QC–QR method, even in the long-range interaction case, is independent of the total number of particles.*

Due to the long-range Coulomb interactions, the displacement in Fig. 11 is quite different from that in Fig. 6 where only the

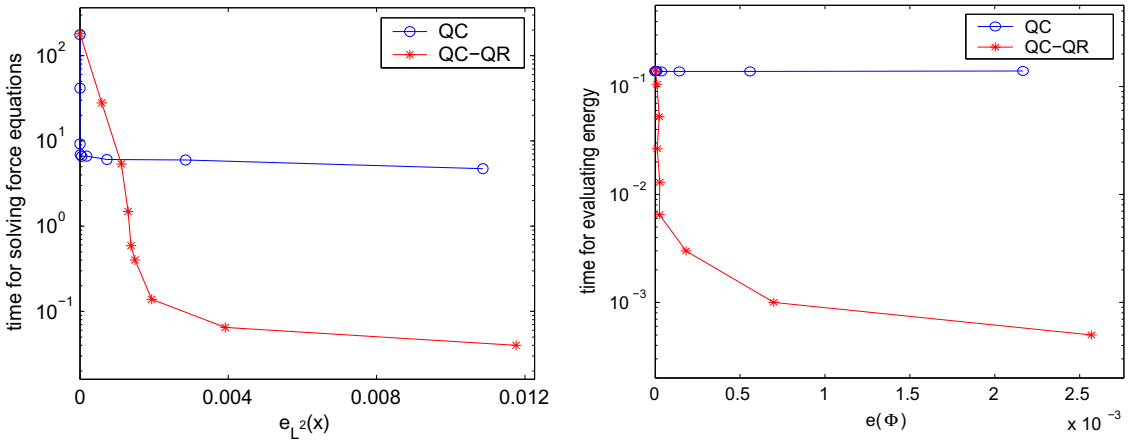

Fig. 9. The errors versus the time used for the corresponding calculation in the short-range interaction cases, where the total number of particles $N = 4096$.

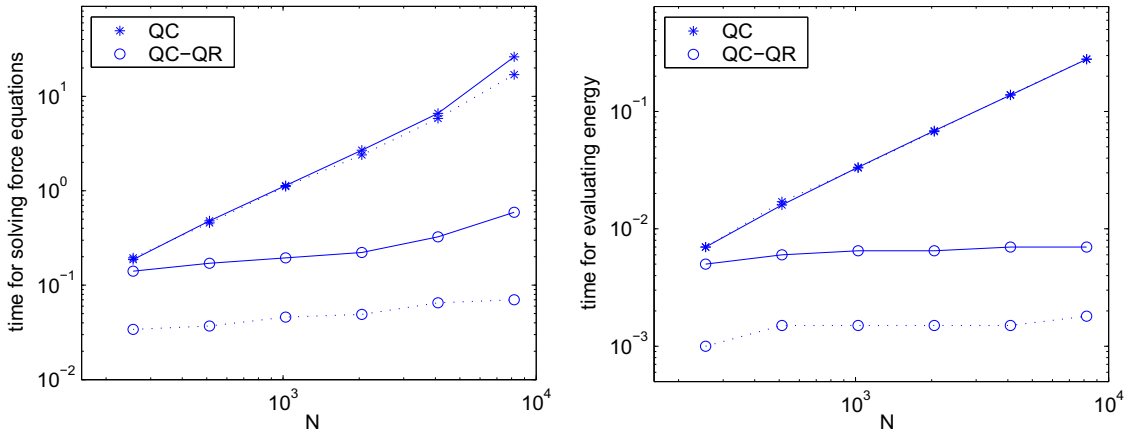

Fig. 10. The time used in solving the force equilibrium equations (left) and in evaluating the energy (right) for different number of particles N in the short-range interaction case; solid line: $\tilde{N}_r = 65$; dashed line: $\tilde{N}_r = 17$.

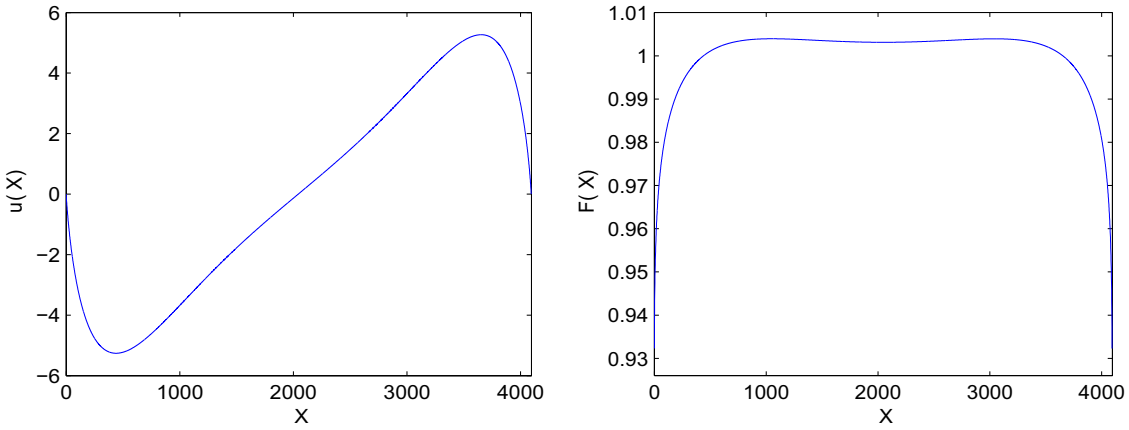

Fig. 11. Displacement (left) and displacement gradient (right) of the monoatomic chain in the long-range interaction case.

Lennard–Jones interatomic potential is applied. In fact, for each particle $\alpha \in \mathcal{N}$, in the close-in region, the interaction is still dominated by the Lennard–Jones potential; this is also indicated by Fig. 5. But, for the far-away region, the dominant force becomes the Coulomb force and it cannot be neglected. Furthermore, since all particles have positive unit charge, the force on particle α due to the interaction with the particles on the same side are all repulsive. Consequently, the particle α may have strong accumulated repulsive forces from both sides. As a result, the position of particle α is determined by the competition between the short-range Lennard–Jones force, the accumulated Coulomb repulsive forces, and the external force.

Again, *to achieve the same error, the QC–QR method needs much less time than the QC method*. For the same number of representative

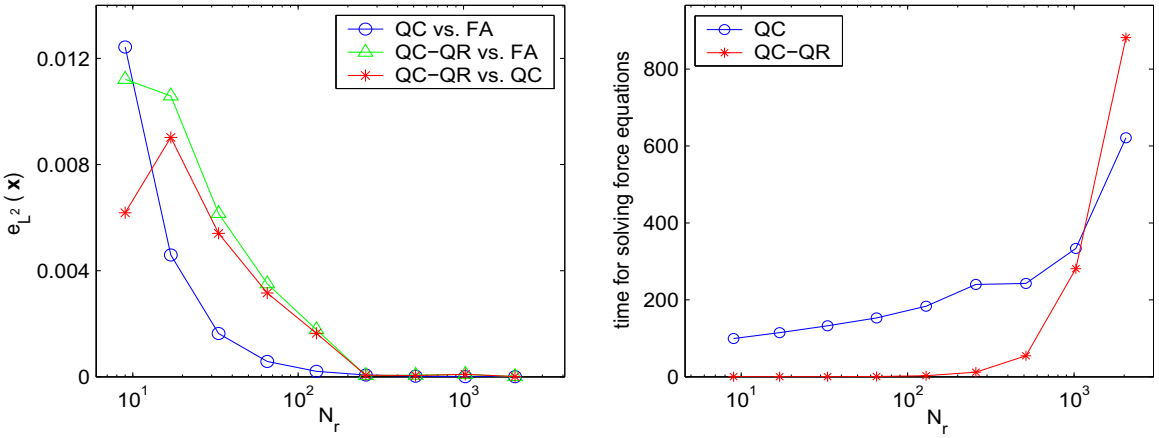

Fig. 12. Position errors (left) and the time used in solving the force equilibrium equations (right) for different numbers of representative particles in the long-range interaction case, where the total number of particles $N = 4096$.

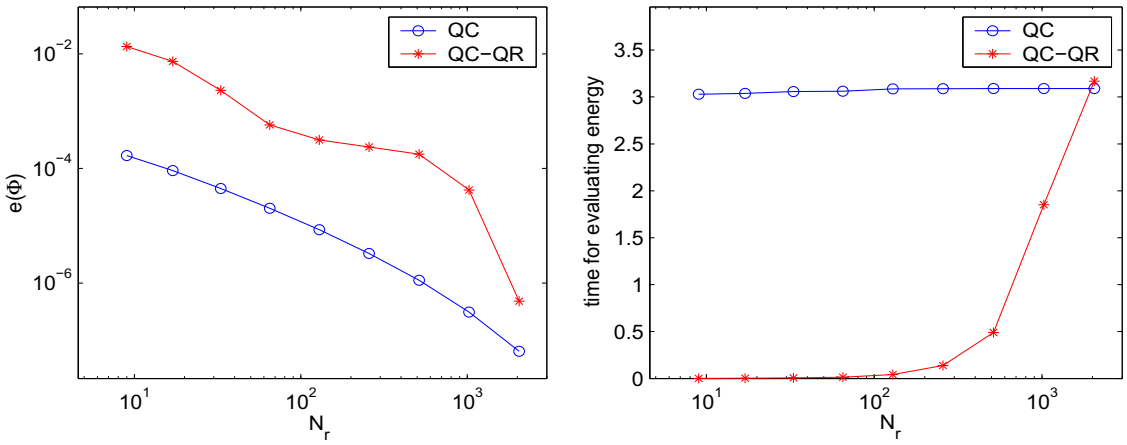

Fig. 13. Relative energy errors (left) and the time used in evaluating energy (right) for different numbers of representative particles in the long-range interaction case, where the total number of particles $N = 4096$.

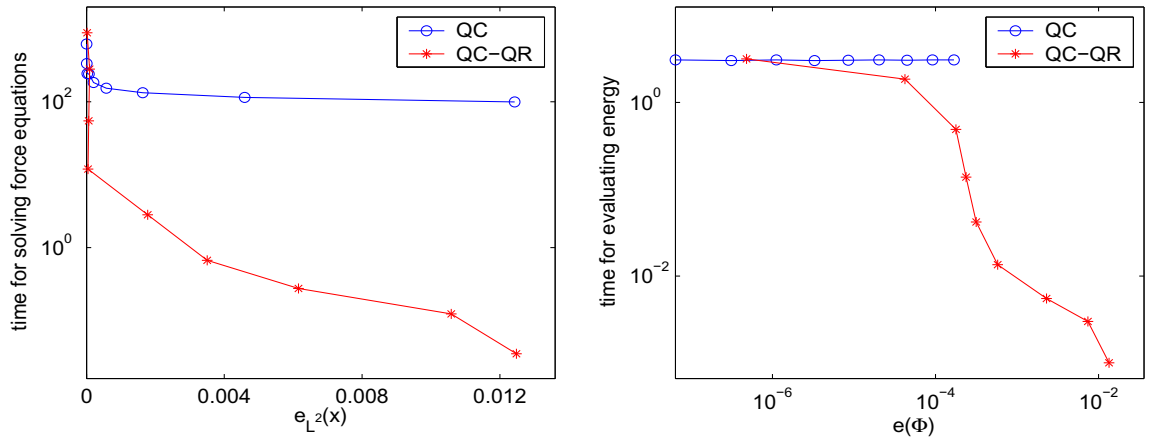

Fig. 14. The errors versus the time used for the corresponding calculation in the long-range interaction cases, where the total number of particles $N = 4096$.

particles, we find that the relative error in energy of the long-range interaction case is bigger than that of the short-range interaction case. This may be caused by the approximation of the interactions from far-away regions. To reduce this error, a higher order quadrature rule can be considered in (3.16), e.g., by choosing $p > 2$ and $q > 2$.

6. Summary and discussion

We have presented quadrature-rule (QC–QR) type approximations to the quasicontinuum (QC) method and illustrated their effectiveness for both short-range and long-range interatomic interaction problems. Compared to the full atomistic method, the

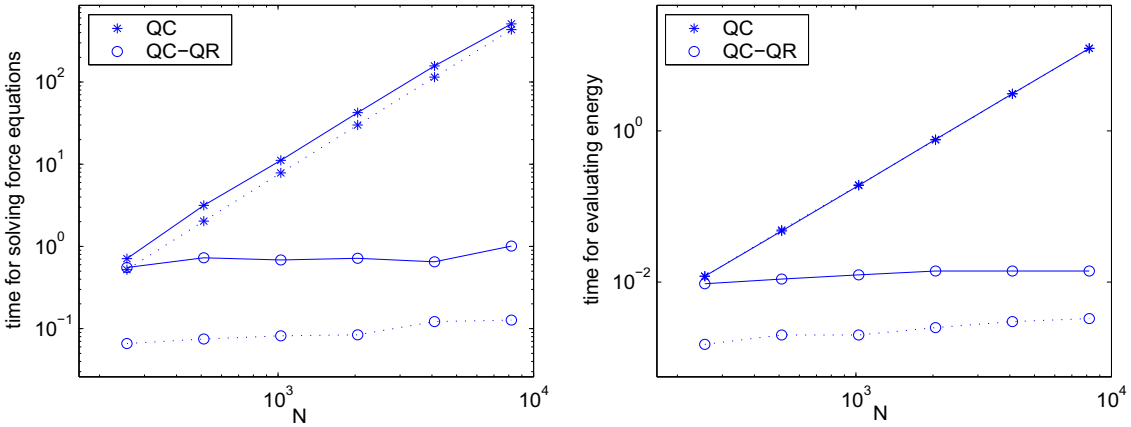

Fig. 15. The time used in solving the force equilibrium equations (left) and in evaluating the energy (right) for different number of particles N in the long-range interaction case; solid line: $\tilde{N}_r = 65$; dashed line: $\tilde{N}_r = 17$.

QC method has fewer degrees of freedom but its computational complexity still depends on N, the total number of particles; in fact, the complexity is of $O(N^2)$. On the other hand, QC–QR methods have computational costs that depend on the number of representative particles but not on the total number of particles. Thus, these methods have much lower computational costs compared to the QC method.

Numerical examples were presented to test the accuracy and efficiency of the QC–QR method. Compared to the QC method, the QC–QR method has sufficient accuracy but its computational time is much shorter than that of the QC method. Especially, the QC–QR type method is much faster when approximating the total energy, and its computational complexity depends on the number of representative particles. The fewer the representative particles, the shorter the computational time needed. In summary, for the same error and for both short and long-range interactions, the QC–QR method is much less costly than the QC method, and also, as is demonstrated in [19], cluster summation approximations of the QC method.

Of course, a much greater array of tests in two and three dimensions are needed to ultimately provide convincing evidence about the efficacy of QC–QR methods; this is the subject of future work.

References

[1] E. Tadmor, R. Phillips, M. Ortiz, Mixed atomistic and continuum models of deformation in solids, Langmuir 12 (1996) 4529–4534.
[2] E. Tadmor, M. Ortiz, R. Phillips, Quasicontinuum analysis of defects in solids, Philos. Mag. A 73 (1996) 1529–1563.
[3] M. Arndt, M. Luskin, Goal-oriented atomistic-continuum adaptivity for the quasicontinuum approximation, Int. J. Multi-Comput. Engrg. 5 (2007) 407–415.
[4] M. Arndt, M. Luskin, Error estimation and atomistic-continuum adaptivity for the quasicontinuum approximation of a Frenkel–Kontorova model, SIAM J. Multiscale Model. Simul. 7 (2008) 147–170.
[5] M. Arndt, M. Luskin, Goal-oriented adaptive mesh refinement for the quasicontinuum approximation of a Frenkel–Kontorova model, Comput. Meth. Appl. Mech. Engrg. 197 (2008) 4298–4306.
[6] M. Dobson, M. Luskin, Analysis of a force-based quasicontinuum approximation, Math. Model. Numer. Anal. 42 (2008) 113–139.
[7] M. Dobson, M. Luskin, Iterative solution of the quasicontinuum equilibrium equations with continuation, J. Sci. Comput. 37 (2008) 19–41.
[8] M. Dobson, M. Luskin, An analysis of the effect of ghost force oscillation on quasicontinuum error, Math. Model. Numer. Anal. 43 (2009) 591–604.
[9] M. Dobson, M. Luskin, R. Elliott, E. Tadmor, A multilattice quasicontinuum for phase transforming materials: cascading Cauchy–Born kinematics, J. Comput.-Aided Mater. Des. 14 (2007) 219–237.
[10] W. E, J. Lu, J. Yang, Uniform accuracy of the quasicontinuum method, Phys. Rev. B 74 (2006) 214115.
[11] W. E, P. Ming, Analysis of the local quasicontinuum method, in: Frontiers and Prospects of Contemporary Applied Mathematics, World Scientific, Singapore, 2005, pp. 18–32.
[12] J. Knap, M. Ortiz, An analysis of the quasicontinuum method, J. Mech. Phys. Solids 49 (2001) 1899–1923.
[13] V. Shenoy, R. Miller, E. Tadmor, D. Rodney, R. Phillips, M. Ortiz, An adaptive finite element approach to atomic-scale mechanics: the quasicontinuum method, J. Mech. Phys. Solids 47 (1999) 611–642.
[14] P. Lin, Convergence analysis of a quasi-continuum approximation for a two-dimensional material without defects, SIAM J. Numer. Anal. 45 (2007) 313–332.
[15] E. Tadmor, R. Miller, The theory and implementation of the quasicontinuum method, Handbook of Materials Modeling, vol. 1, Kluwer Academic Publishers, 2005.
[16] R. Miller, E. Tadmor, The quasicontinuum method: overview, applications and current directions, J. Comput.-Aided Mater. Des. 9 (2002) 203–239.
[17] R. Miller, E. Tadmor, R. Phillips, M. Ortiz, Quasicontinuum simulation of fracture at the atomic scale, Model. Simul. Mater. Sci. Engrg. 6 (1998) 607–638.
[18] J. Knap, M. Ortiz, Effect of indenter-radius size on Au(001) nanoidentation, Phys. Rev. Lett. 90 (2003) 226102.
[19] M. Gunzburger, Y. Zhang, A quadrature-rule type approximation to the quasicontinuum method, SIAM J. Multiscale Model. Simul. (in press).
[20] D. Negrut, M. Anitescu, A. El-Azab, P. Zapol, Quasicontinuum-like reduction of density functional theory calculations of nanostructures, J. Nanosci. Nanotechnol. 8 (2007) 1–12.
[21] X. Din, E. Michaelides, Calculation of long-range interactions in molecular dynamics and Monte Carlo simulations, J. Phys. Chem. A 101 (1997) 4322–4331.
[22] N. English, J. MacElroy, Atomistic simulations of liquid water using Lekner electrostatics, Mol. Phys. 100 (2002) 3753–3769.
[23] N. English, Molecular dynamics simulations of microwave effects on water using different long-range electrostatics methodologies, Mol. Phys. 104 (2006) 243–253.
[24] M. Tuckerman, J. Berne, G. Martyna, Molecular dynamics algorithm for multiple time scales: systems with long range forces, J. Chem. Phys. 94 (1991) 6811–6815.
[25] T. Hughes, The Finite Element Method: Linear Static and Dynamic Finite Element Analysis, Prentice-Hall, 1987.
[26] V. Bulatov, W. Cai, Computer Simulations of Dislocations, Oxford University Press, 2006.
[27] J. Lennard-Jones, A. Devonshire, Critical and cooperative phenomena III. A theory of melting and the structure of liquids, Proc. R. Soc. Lond. A 169 (1939) 317–338.